# Magnetic field effect on Poiseuille flow and heat transfer of carbon nanotubes along a vertical channel filled with Casson fluid

Sidra Aman, Ilyas Khan, Zulkhibri Ismail, Mohd Zuki Salleh, Ali Saleh Alshomrani, and Metib Said Alghamdi

Citation: AIP Advances **7**, 015036 (2017); doi: 10.1063/1.4975219
View online: http://dx.doi.org/10.1063/1.4975219
View Table of Contents: http://aip.scitation.org/toc/adv/7/1
Published by the American Institute of Physics

# Magnetic field effect on Poiseuille flow and heat transfer of carbon nanotubes along a vertical channel filled with Casson fluid

Sidra Aman,[1] Ilyas Khan,[2,a] Zulkhibri Ismail,[1] Mohd Zuki Salleh,[1] Ali Saleh Alshomrani,[3] and Metib Said Alghamdi[4]
[1]*Futures and Trends Research Group, Faculty of Industrial Science and Technology, Universiti Malaysia Pahang, Lebuhraya Tun Razak, 26300 UMP Kuantan, Pahang, Malaysia*
[2]*Basic Engineering Sciences Department, College of Engineering, Majmaah University, Majmaah 11952, Saudi Arabia*
[3]*Department of Mathematics, Faculty of Science, King Abdul Aziz University, Jeddah, Saudi Arabia*
[4]*Department of Mathematics, Faculty of Sciences, Jazan University, Saudi Arabia*

(Received 2 November 2016; accepted 11 January 2017; published online 27 January 2017)

Applications of carbon nanotubes, single walls carbon nanotubes (SWCNTs) and multiple walls carbon nanotubes (MWCNTs) in thermal engineering have recently attracted significant attention. However, most of the studies on CNTs are either experimental or numerical and the lack of analytical studies limits further developments in CNTs research particularly in channel flows. In this work, an analytical investigation is performed on heat transfer analysis of SWCNTs and MWCNTs for mixed convection Poiseuille flow of a Casson fluid along a vertical channel. These CNTs are suspended in three different types of base fluids (Water, Kerosene and engine Oil). Xue [Phys. B Condens. Matter **368**, 302–307 (2005)] model has been used for effective thermal conductivity of CNTs. A uniform magnetic field is applied in a transverse direction to the flow as magnetic field induces enhancement in the thermal conductivity of nanofluid. The problem is modelled by using the constitutive equations of Casson fluid in order to characterize the non-Newtonian fluid behavior. Using appropriate non-dimensional variables, the governing equations are transformed into the non-dimensional form, and the perturbation method is utilized to solve the governing equations with some physical conditions. Velocity and temperature solutions are obtained and discussed graphically. Expressions for skin friction and Nusselt number are also evaluated in tabular form. Effects of different parameters such as Casson parameter, radiation parameter and volume fraction are observed on the velocity and temperature profiles. It is found that velocity is reduced under influence of the exterior magnetic field. The temperature of single wall CNTs is found greater than MWCNTs for all the three base fluids. Increase in volume fraction leads to a decrease in velocity of the fluid as the nanofluid become more viscous by adding CNTs.  [http://dx.doi.org/10.1063/1.4975219]

## I. INTRODUCTION

Non-Newtonian fluids have immense applications in industries such as chemicals, cosmetics, pharmaceuticals. They are attracted for scientists due to their wide applications. Navier Stokes theory is inadequate for such fluids and no single equation can exhibit the properties of all fluids. Thus a number of non-Newtonian fluid models are introduced to explain the characteristics of such fluids. Some of them are power law, second grade, third grade, fourth grade, Brinkman type, micropolar,

[a]Corresponding author email: ilyaskhanqau@yahoo.com/i.said@mu.edu.sa h/p: 009660503346170.

 

Jaffery, Walters' B, Maxwell, Oldroyd-B, Burgers and generalized Burgers models. However, there is another popular model namely, Casson model. Casson[1] introduced this model for the first time to predict flow behavior of pigment oil suspensions of the printing ink type. Casson fluid is a shear thinning liquid which is assumed to have infinite viscosity at zero rate of shear, a yield stress below which no flow occurs, and a zero viscosity at an infinite rate of shear.[2] Examples of Casson fluids are jelly, tomato sauce, honey, soup and human blood. Eldabe and Salwa[3] have studied the Casson fluid for the flow between two rotating cylinders. Boyed *et al.*[4] investigated the Casson fluid flow for the steady and oscillatory blood flow. Swati *et al.*[5] surveyed numerically Casson fluid flow over an unsteady stretching surface. Pramanik[6] studied Casson fluid flow and heat transfer past an exponentially porous stretching surface in the presence of thermal radiation. Noreen[7] analyzed the influence of magnetic field on peristaltic flow of a Casson fluid in an asymmetric channel. Farhad *et al.*[8] studied closed form solutions for unsteady free convection flow of a second grade fluid over an oscillating vertical plate. Hussanan *et al.*[9] investigated the unsteady boundary layer flow and heat transfer of Casson fluid over an oscillating plate with Newtonian heating. Asma *et al.*[10] studied unsteady magnetohydrodynamic (MHD) free convection flow of Casson fluid past an oscillating vertical plate embedded in a porous medium. Imran *et al.*[11] studied the effects of slip on free convection flow of Casson fluid over an oscillating vertical plate. Heat and mass transfer in Casson fluid over an exponentially permeable stretching surface was studied by Raju *et al.*[12] They presented dual solutions to the problem by comparing the results of Casson fluid with Newtonian fluid numerically by using Matlab bvp4c package. Gentile et al.[13] investigated the transport of nanoparticles in blood vessels with blood considered as Casson fluid (the effect of vessel permeability and blood Rheology), hence contributing in biomedical engineering. Rizwan *et al.*[14] studied convective heat transfer and MHD effects on Casson nanofluid flow over a shrinking sheet by taking suction/injection effect on the wall. Siddiqui *et al.*[15] developed a mathematical model to study the transport mechanism of a Casson fluid flow due to metachronal beating of cilia in a cylindrical tube. Nadeem *et al.*[16] investigated MHD three-dimensional boundary layer flow of Casson nanofluid past a linearly stretching sheet with convective boundary condition. MHD stagnation-point flow of Casson fluid and heat transfer over a stretching sheet with thermal radiation was investigated by Krishnendu.[17] Reynolds number impact on the flow of electro rheological fluid of a Casson type between fixed sheets of revolution was discussed by Walicka and Falicki.[18] The effect of magnetic field and heat source on the steady boundary layer flow and heat transfer of a Casson nanofluid past a vertical exponentially stretching cylinder across its radial direction was discussed by Sarojamma and Vendabai.[19] Mustafa and Junaid[20] proposed a model for flow of Casson nanofluid past a non-linearly stretching sheet considering magnetic field effects.

Nanofluids are fluids containing nanometer-sized materials called nanoparticles. These fluids are used in order to enhance the thermal conductivity and heat transfer rate of base fluids. Different types of nanoparticles of different shapes and sizes are used for this purpose. The nanoparticles used in nanofluids are usually made of metals, oxides, carbides, or carbon nanotubes (CNTs). Common base fluids where nanoparticles are usually suspended include water, ethylene glycol and engineoil. CNTs used in nanofluids are typically of two types namely single walls carbon nanotubes (SWCNTs) and multiple walls carbon nanotubes (MWCNTs) as shown in figure 1.

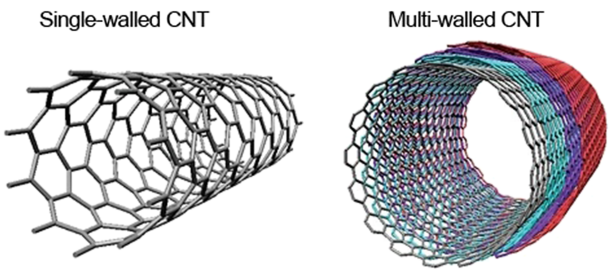


FIG. 1. Single and multiple walls carbon nanotubes.

As compared to other nanostructure materials, CNTs have got the highest conductivity enhancement, opening the door to a wide range of nanotube applications, including use in nanofluids. Their thermal conductivity is much higher than the thermal conductivity of metal nanoparticles or metal oxide nanoparticles. Due to cylindrical carbon molecules origin, CNTs have exceptional mechanical, thermal, electrical and optical properties. They have special thermal properties with very high thermal conductivities. The diameter of CNTs ranges from 1 to 100 nm and lengths in micrometer. They have two hundred times strength and five times elasticity of steel, fifteen times thermal conductivity and 1000 times current capacity of copper. Besides that CNTs are declared the non-hazardous particles for the environment by environmental protection agency. Therefore, these days the researchers are concentrating more on CNTs research to enhance the thermal conductivity as compare to other nanoparticles fluids. Liu *et al.*[21] studied the enhancement of thermal conductivity of ethylene glycol and synthetic engine oil in the presence of MWCNTs. They found that CNTs-ethylene glycol suspensions have higher thermal conductivities than ethylene glycol fluid without CNTs. Similar result was obtained in case of synthetic engine oil. For CNTs-ethylene glycol suspension at a volume fraction of 0.01, thermal conductivity is increased by 12.4% while for CNTs-synthetic engine oil by 30% at a volume fraction of 0.02.Marquis and Chibnate[22] investigated that both types of CNTs (SWCNT and MWCNTs) increased the thermal conductivity of nanofluids and nanolubricants. They used three different types of nanofluids and nanolubricants in their study. The effects of concentration of CNTs and temperature on effective thermal conductivity were investigated by Wen and Ding.[23] It was found that effective thermal conductivity increased with increasing concentration of CNTs. Xie et al.[24] studied experimentally the nanofluids containing MWCNTsand their enhanced conductivities. As expected, theyfound that the addition of CNTs into a fluid leads to enhancement of thermal conductivity. The thermal conductivity enhancement increases with the increase in nanotubes loading. Hone[25] and Antar *et al.*[26] reported that for SWCNTs the thermal conductivity is upto 6,600 W/mK and for MWCNTs is upto 3,000 W/mK.Water driven flow of CNTs in a rotating channel has been investigated by Hussain *et al.*[27] They observed that SWCNTs show less resistance to the fluid flow as compared to MWCNTs. Khan *et al.*[28] studied fluid flow and heat transfer of CNTs along a flat plate with Navier slip boundary condition. They found that water-based CNTs have higher densities and thermal conductivities than kerosene and engine oil-based CNTs. The reason for this is the higher thermal conductivity and density of water. Haq *et al.*[29] studied water based flow in the presence of SWCNT and MWCNT, they observed a higher skin friction and Nusselt number for SWCNT compare to MWCNT. In another study, Haq *et al.*[30] showed that engine oil based CNT fluid has higher skin friction and heat transfer rate as compared to water and kerosene based CNT fluid.

Recently an immense attention has been paid on coating CNTs on textile fabrics in the field of textile. Another application of CNTs is that in acoustics such as loudspeakers and earphone. Xiao *et al.*[31] found that very thin CNTs films could emit loud sounds, hence they made practical CNT thin film loudspeakers. They have been suggested as promising absorbents for removal of contaminant in water and wastewater treatment systems. Camilli *et al.*[32] proposed a three-dimensional carbon nanotube network for water treatment. They demonstrated that a 3-dimensional structure uptakes masses of toxic organic solvent from water about 3.5 times higher than the absorbed by individual CNTs. Moreover, they have a high oil-absorption capacity than the CNT sponges. Halelfadel *et al.*[33] investigated viscosity of carbon nanotubes water based-nanofluids. They presented experimental result on viscosity of carbon nanotubes considering the influence of temperature and volume fraction. In another study, Halelfadel *et al.*[34] worked on the efficiency of carbon nanotubes water based nanofluids as coolants. They investigated the effect of low nanoparticles volume fraction (ranging from 0.0055% to 0.278%) on density, thermal conductivity and viscosity of nanofluids.

Kamali and Binesh[35] numerically investigated the convective heat transfer of multi wall CNTs-based nanofluids in a straight tube under constant wall heat flux condition. They found that the heat transfer coefficient is dominated by the wall region due to non-Newtonian behavior of CNT nanofluid. Meyer *et al.*[36] investigated experimentally the convective heat transfer enhancement of aqueous suspensions of multi-walled CNTs flowing through a straight horizontal tube. They determined the heat transfer coefficients and friction factors are Reynolds number dependent. More exactly, they found that heat transfer was enhanced when comparing the data on a Reynolds Nusselt graph and the increase in viscosity was four times the increase in the thermal conductivity. Kandasamy *et al.*[37]

studied the impact of chemical reaction on Cu, Al2O3, and SWCNTs-nanofluid flow under the slip conditions numerically by using Runge-Kutta-Fehlberg Method with shooting technique. Marangoni convection flow and heat transfer characteristics of water-CNT nanofluid droplets was proposed by Al-Sharafi *et al.*[38] Kandasamy *et al.*[39] studied single walled carbon nanotubes on MHD unsteady flow over a porous wedge with thermal radiation with variable stream condition. Xue[40] presented a model for the effective thermal conductivity of carbon nanotube composites. Their model predicts that large length of CNTs plays a key role in the enhancement of their thermal conductivity. Jiang *et al.*[41] in their experimental work, used CNTs of different diameters and lengths and tested their effect on thermal conductivities. They found that larger the aspect ratio, larger will be the thermal conductivity. An interesting result was found that thermal conductivity of CNTs with smaller diameter is higher than those of larger diameter.

Mixed convection occurs in many industrial and technological processes such as chemical processing, nuclear reactors, pollution control in buildings and thermal insulations. X-Hong Ren *et al.*[42] studied combined convective heat and airborne pollutant removals in a slot vented enclosure under different flow schemes. MHD mixed convection flow in a linearly heated cavity was analyzed by Al-Salem *et al.*[43] For other studies on mixed convection heat transfer the reader is referred to the references 44–50.

Applications of CNTs in thermal engineering have recently attracted significant attention. However, most of the studies on CNTs are either experimental or numerical and the lack of analytical studies limits further developments in CNTs research particularly in channel flows. From the literature review, it is found that no study has been reported on analytical work for heat transfer analysis of CNTs Casson fluid. In this direction, even numerical or experimental studies for Casson fluid are not available. This work will not only provide a pioneering study but will also help the numerical or experimental investigators to compare their studies with the results reported in this work.

This work aims to study heat transfer analysis in Poiseuille flow of carbon nanotubes (SWCNTs and MWCNTs) with Casson fluid in a vertical channel. The flow is affected by the magnetization of the fluid under the influence of an external magnetic field. The equations are formulated and then transformed to non-dimensionless form. Perturbation method is applied to find the analytical solution of velocity and temperature fields. At the end, skin friction and Nusselt number are evaluated.

## II. THEORETICAL MODELS FOR EFFECTIVE THERMAL CONDUCTIVITIES

Many theoretical models are available in literature, which can be used to predict the effective thermal conductivity enhancement of CNTs suspensions. Maxwell[51] proposed an explicit relation for the effective thermal conductivity in terms of the thermal conductivity ratio $\sigma = \frac{k_{CNT}}{k_f}$, and the volume fraction $\phi$ :

$$\frac{k_{nf}}{k_f} = 1 + \frac{3(\sigma - 1)\phi}{(\sigma + 2) - (\sigma - 1)\phi}. \tag{1}$$

Jeffery[52] and Davis[53] proposed the following two theoretical models for higher order of volume fractions:

$$\frac{k_{nf}}{k_f} = 1 + 3\lambda\phi + (3\lambda^2 + \frac{3\lambda^2}{4} + \frac{9\lambda^3}{16}\frac{\sigma + 2}{2\sigma + 3} + .....)\phi^2, \tag{2}$$

$$\frac{k_{nf}}{k_f} = 1 + \frac{3(\sigma - 1)\phi}{(\sigma + 2) - (\sigma - 1)\phi}\{\phi + \phi(\sigma)\phi^2 + O(\phi^3)\}, \tag{3}$$

respectively, where $\lambda = (\sigma - 1)/(\sigma + 2)$. The higher order terms represent pair interactions of randomly dispersed spheres. The above three models give identical predictions of the effective thermal conductivity for low-volume fractions. However those models do not account for the shape factor of the particles. Hamilton and Crosser[54] developed a theoretical model which accounts for the shapes factor of the particles:

$$\frac{k_{nf}}{k_f} = \frac{\sigma + (n - 1) - (n - 1)(1 - \sigma)\phi}{\sigma + (n - 1) + (1 - \sigma)\phi}, \tag{4}$$

TABLE I. Conventional models for effective thermal conductivities of solid/liquid suspensions.

| Models | Expressions | Remarks |
|---|---|---|
| Maxwell | $\frac{k_{nf}}{k_f} = 1 + \frac{3(\sigma-1)\phi}{(\sigma+2)-(\sigma-1)\phi}$. | i) Spherical particles are considered. ii) Accurate to $\phi^1$, applicable to $\phi < 1$ |
| Jeffery | $\frac{k_{nf}}{k_f} = 1 + 3\lambda\phi + (3\lambda^2 + \frac{3\lambda^2}{4} + \frac{9\lambda^3}{16}\frac{\sigma+2}{2\sigma+3} + .....)\phi^2$ | iii) Accurate to order $\phi^2$; higher order terms represent pair interactions of randomly dispersed spheres. |
| Devis | $\frac{k_{nf}}{k_f} = 1 + \frac{3(\sigma-1)\phi}{(\sigma+2)-(\sigma-1)\phi}\{\phi + \phi(\sigma)\phi^2 + O(\phi^3)\}$ | i) Accurate to order $\phi^2$; higher order terms represent pair interactions of randomly dispersed spheres. ii) $f(\sigma) = 2.5$ for $\sigma = 10$ ; $f(\sigma) = 0.5$ for $\sigma = \infty$ |
| Hamilton and Crosser | $\frac{k_{nf}}{k_f} = \frac{\sigma+(n-1)-(n-1)(1-\sigma)\phi}{\sigma+(n-1)+(1-\sigma)\phi}$ | i) Spherical and non-spherical particles are considered: n=3 for spheres, n=6 for cylinders. ii) Accurate to $\phi^1$,applicable to $\phi < 1$ |

where $n$ is the shape factor of the particle given by $n = \frac{3}{\varphi^\omega}$, where $\varphi = 1$ for spheres and 0.5 for cylinders and $\omega$ ranges from 1 to 2. Hamilton and Crosser (HC) model reduces to Maxwell model when $\varphi = 1$. Choi[55] shows that for cylindrical shape nanoparticles HC underestimate the experimental results by comparing measurements to the existing theoretical predictions. The enhancement of thermal conductivity is 160 % for 1% vol nanotubes in oil, while that is by theoretical model are not more than 10% as listed in Table I.

Xue[40] observed that the existing models are only valid for spherical or rotational elliptical particles with small axial ratio. Another limitation of those models is that they do not account for the effect of space distribution of CNTs on thermal conductivity. He proposed a theoretical model based on Maxwell theory considering rotational elliptical nanotubes with very large axial ratio and compensating the effects of the space distribution on CNTs

$$\frac{k_{nf}}{k_f} = \frac{1-\phi+2\phi\left(\frac{k_{CNT}}{k_{CNT}-k_f}\right)\ln\frac{k_{CNT}+k_f}{2k_f}}{1-\phi+2\phi\left(\frac{k_f}{k_{CNT}-k_f}\right)\ln\frac{k_{CNT}+k_f}{2k_f}}. \tag{5}$$

We used Xue[40] model to predict thermal conductivity and dimensionless heat transfer rate of nanofluids in our study. We will solve the proposed model analytically by using perturbation technique. In the end, we will present the physical interpretation of our results.

## III. FORMULATION AND SOLUTION OF THE PROBLEM

Consider MHD flow in a vertical channel of width $a$, with static walls at $y = 0$ and $y = a$, with heat transfer in a Casson fluid (three different fluids i.e. Water, Engine oil, Kerosene oil-based nanofluids) containing SWCNTs and MWCNTs. The flow is assumed to be incompressible and unsteady. A uniform magnetic field of strength $B_0$ is applied in a perpendicular direction to the flow (along $x$-axis). Mixed convection is generated by external pressure gradient together with buoyancy force. The viscous dissipation effect is neglected in the energy equation. In vertical channel, $T_0$ and $T_a$ show lower and upper plate temperatures. The Reynolds number is assumed small. The governing equations of momentum and energy are as under:

$$\rho_{nf}\frac{\partial u}{\partial t} = -\frac{\partial p}{\partial x} + \mu_{nf}\left(1+\frac{1}{\beta}\right)\frac{\partial^2 u}{\partial y^2} - \sigma_{nf}B_0^2 u + (\rho\beta_T)_{nf}\, g\,(T - T_a), \tag{6}$$

$$(\rho c_p)_{nf}\frac{\partial T}{\partial t} = k_{nf}\frac{\partial^2 T}{\partial y^2} - \frac{\partial q_r}{\partial y}, \tag{7}$$

where $u = u(y, t), T = T(y, t)$ , $\rho_{nf}$ , $\mu_{nf}$, $\sigma_{nf}$, $\beta_T g$ , $\left(\rho c_p\right)_{nf}$ , $k_{nf}$ , $q_r$ , are respectively fluid velocity in the x− direction, temperature, density, the dynamic viscosity, electrical conductivity of the base fluid, volumetric thermal expansion coefficient, gravitational acceleration, heat capacitance of nanofluids, thermal conductivity of nanofluid and radiative heat flux.
The corresponding boundary conditions are:

$$u(0,\ t) = 0, \quad u(a,\ t) = 0, \tag{8}$$

$$T(0, t) = T_0, \quad T(a,\ t) = T_a. \tag{9}$$

The external pressure gradient in the flow direction is taken as $-\partial p/\partial x = \lambda\varepsilon exp(i\omega t)$, where $\lambda$ is constant and $\omega$ is the oscillation frequency. As in the following, Xue model[40] is used in this problem for thermal conductivity and dynamic viscosity.

$$\mu_{nf} = \frac{\mu_f}{(1-\phi)^{2.5}}, \tag{10}$$

$$\frac{k_{nf}}{k_f} = \frac{1-\phi+2\phi\left(\frac{k_{CNT}}{k_{CNT}-k_f}\right)\ln\frac{k_{CNT}+k_f}{2k_f}}{1-\phi+2\phi\left(\frac{k_f}{k_{CNT}-k_f}\right)\ln\frac{k_{CNT}+k_f}{2k_f}}. \tag{11}$$

The density $\rho_{nf}$, thermal expansion coefficient $(\rho\beta)_{nf}$ , heat capacitance$\left(\rho c_p\right)_{nf}$ , thermal conductivity $\sigma_{nf}$, are derived by using the relations given by Refs. 20 and 37.

$$\rho_{nf} = (1-\phi)\rho_f + \phi\rho_{CNT},\ (\rho\beta)_{nf} = (1-\phi)(\rho\beta)_f + \phi(\rho\beta)_{CNT}$$
$$\left(\rho c_p\right)_{nf} = (1-\phi)(\rho c_p)_f + \phi(\rho c_p)_{CNT},\ \sigma_{nf} = \sigma_f\left(1 + \frac{3(\sigma-1)\phi}{(\sigma+2)-(\sigma-1)\phi}\right), \tag{12}$$

where $\phi$ is the nanoparticles volume fraction, $\rho_f$ and $\rho_{CNT}$ is the density of the base fluid and CNTs, the volumetric coefficient of thermal expansions of carbon nanotubes and base fluids are denoted by $\beta_{CNT}$ and $\beta_f$ respectively, $(c_p)_{CNT}$ and $(c_p)_f$ is the specific heat capacities of CNTs and base fluids at constant pressure.
The radiative heat flux is given by:

$$\frac{\partial q_r}{\partial y} = -4\alpha^2(T - T_a), \tag{13}$$

where $\alpha$ is the radiation absorption coefficient.
Substituting Eq. (13) into Eq. (7) yields:

$$(\rho c_p)_{nf}\frac{\partial T}{\partial t} = k_{nf}\frac{\partial^2 T}{\partial y^2} + 4\alpha^2(T - T_a). \tag{14}$$

Introducing the following dimensionless quantities

$$x^* = \frac{x}{d},\ y^* = \frac{y}{d},\ u^* = \frac{u}{U_0},\ t^* = \frac{tU_0}{d},\ p^* = \frac{d}{\mu U_0}p,$$
$$T^* = \frac{T - T_a}{T_0 - T_a},\ \omega^* = \frac{d\omega}{U_0},\quad -\frac{\partial p^*}{\partial x^*} = \lambda\varepsilon exp\left(i\omega^* t^*\right). \tag{15}$$

into Eqs. (6, 7, 8, 9 and 14) and in view of the above relations, we get (∗ Symbol is dropped for convenience)

$$a_o\frac{\partial u}{\partial t} = \lambda\varepsilon\exp(i\omega t) + a_1\frac{\partial^2 u}{\partial y^2} - a_2 u - a_3 T, \tag{16}$$

$$u(0,t)=0,\quad u(1,t)=0\,, \tag{17}$$

$$b_0^2\frac{\partial T}{\partial t}=\frac{\partial^2 T}{\partial y^2}+b_1^2 T, \tag{18}$$

$$T(0,t)=1,\quad T\,(1,t)=0, \tag{19}$$

where

$$\phi_2=\frac{1}{(1-\phi)^{2.5}},\quad ,\phi_3=\left(1+\frac{3\,(\sigma-1)\,\phi}{(\sigma+2)-(\sigma-1)\,\phi}\right),$$
$$\phi_4=(1-\phi)+\frac{\phi\,(\rho\beta_T)_{CNT}}{(\rho\beta_T)_f},\quad \phi_5=(1-\phi)+\phi\frac{\left(\rho c_p\right)_s}{\left(\rho c_p\right)_f}$$
$$\mathrm{Re}=\frac{U_0 d\rho}{\mu_f}\quad ,\quad M=\delta\beta_0^2\frac{d^2}{\mu_f}\quad ,\quad Gr=\frac{gd\,(\beta_T)_f\,(T_0-T_a)}{U_0^2}\quad ,$$
$$Pe=\frac{U_0 d\left(\rho c_p\right)_f}{k_f}\,,\ N^2=\frac{4\alpha^2 d^2}{k_f}\,,\ b_1^2=\frac{N^2}{\lambda_{nf}},\ \ \lambda_{nf}=\frac{k_{nf}}{k_f}\,,a_0=\phi_1\,\mathrm{Re},$$
$$a_1=\phi_2\left(1+\frac{1}{\beta}\right),\ \ a_2=\phi_3 M\ ,b_0^2=\frac{\phi_5 Pe}{\lambda_{nf}},Ri=\frac{\left(\rho c_p\right)_f U_0 d}{k_f}, \tag{20}$$

Here $Re$, $M$, $Gr$, $Pe$, $N$, $Ri$ are the Reynolds number, the magnetic parameter, the thermal Grashoff number, Peclet number and the radiation parameter and Richardson number respectively. For the sake of simplification other constants are used as in Eq. (20).

In order to solve Eqs. (16) and (18) with boundary conditions (17) and (19), the perturbed solutions for velocity and temperature are taken of the forms:

$$u(y,t)=\left[u_0(y)+\varepsilon\exp(i\omega t)u_1(y)\right], \tag{21}$$

$$T(y,t)=\left[T_0(y)+\varepsilon\exp(i\omega t)T_1(y)\right]. \tag{22}$$

Using Eqs. (16)-(19) into(21) and(22) we have the following system of ordinary differential equations:

$$\frac{d^2u_0(y)}{dy^2}-a_4^2u_0(y)=-\frac{a_3}{a_1}T_0(y)\,, \tag{23}$$

$$u_0(0)=0,\quad u_0(1)=0\,, \tag{24}$$

$$\frac{d^2u_1(y)}{dy^2}-a_5^2u_1(y)=-\frac{\lambda}{a_1}\,, \tag{25}$$

$$u_1(0)=0,\quad u_1(1)=0\,, \tag{26}$$

$$\frac{d^2T_0(y)}{dy^2}+b_1^2T_0(y)=0\,, \tag{27}$$

$$T_0(0)=1\ \ ,\ \ T_0(1)=0\ , \tag{28}$$

$$\frac{d^2T_1(y)}{dy^2}+b_2^2T_1(y)=0\,, \tag{29}$$

$$T_1(0)=0\,,\quad T_1(1)=0, \tag{30}$$

where

$$a_4^2 = \frac{a_2}{a_1}, \quad a_5^2 = \left(\frac{a_2 + a_0 i\omega}{a_1}\right), \quad b_2^2 = \left(b_1^2 - b_0^2 i\omega\right). \tag{31}$$

Solutions of Eqs. (27) and (29) under boundary conditions (28) and (30), yield to

$$T_0(y) = \left[-\frac{\cos b_1 \sin b_1 y}{\sin b_1} + \cos b_1 y\right], \tag{32}$$

$$T_1(y) = 0. \tag{33}$$

Eq. (22) using Eqs. (32) and (33) gives

$$T(y) = \left[-\frac{\cos b_1 \sin b_1 y}{\sin b_1} + \cos b_1 y\right]. \tag{34}$$

Equations (23) and (25) under boundary conditions (24) and (26), give:

$$u_0(y) = c_5 \sinh a_4 y + c_6 \cosh a_4 y - \frac{a_3}{a_1\left(b_1^2 + a_4^2\right)}\left(\cos b_1 \sin b_1 y - \cos b_1 y\right), \tag{35}$$

$$u_1(y) = c_7 \sinh a_5 y + c_8 \cosh a_5 y + \frac{\lambda}{a_1 a_5^2}, \tag{36}$$

which results in

$$u_0(y) = \frac{a_3 \cosh a_4 \sinh a_4 y}{a_1 \sinh a_4\left(b_1^2 + a_4^2\right)} - \frac{a_3 \cosh a_4 y}{a_1\left(b_1^2 + a_4^2\right)} - \frac{a_3}{a_1\left(b_1^2 + a_4^2\right)}\left(\frac{\cos b_1 \sin b_1 y}{\sin b_1} - \cos b_1 y\right), \tag{37}$$

$$u_1(y) = \left[\frac{\lambda sinh a_5 y}{a_1 a_5^2 sinh a_5}(cosh a_5 - 1) - \frac{\lambda}{a_1 a_5^2} cosh a_5 y + \frac{\lambda}{a_1 a_5^2}\right], \tag{38}$$

with arbitrary constants

$$c_5 = \frac{a_3 \cosh a_4}{a_1 \sinh a_4\left(b_1^2 + a_4^2\right)}, \quad c_6 = \frac{a_3}{a_1\left(b_1^2 + a_4^2\right)},$$
$$c_7 = \frac{\lambda}{a_1 a_5^2 \sinh a_5}(\cosh a_5 - 1), \quad c_8 = -\frac{\lambda}{a_1 a_5^2}. \tag{39}$$

Finally, substituting Eqs. (37)–(38) into Eq. (21) gives:

$$u(y,t) = \frac{a_3 \cosh a_4 \sinh a_4 y}{a_1 \sinh a_4\left(b_1^2 + a_4^2\right)} - \frac{a_3 \cosh a_4 y}{a_1\left(b_1^2 + a_4^2\right)} - \frac{a_3}{a_1\left(b_1^2 + a_4^2\right)}\left(\frac{\cos b_1 \sin b_1 y}{\sin b_1} - \cos b_1 y\right)$$
$$+ \varepsilon \exp(i\omega t)\left[\frac{\lambda \sinh a_5 y}{a_1 a_5^2 \sinh a_5}(\cosh a_5 - 1) - \frac{\lambda}{a_1 a_5^2}\cosh a_5 y + \frac{\lambda}{a_1 a_5^2}\right]. \tag{40}$$

## IV. SKIN FRICTION AND NUSSELT NUMBER

Skin friction and Nusselt number are evaluated from Eqs. (34) and (40) as:

$$c_f(t) = \frac{a_3 a_4 \cosh a_4}{a_1 \sinh a_4\left(b_1^2 + a_4^2\right)} - \frac{a_3 b_1 \cos b_1}{a_1\left(b_1^2 - a_4^2\right)} + \varepsilon \exp(i\omega t)\left[\frac{\lambda}{a_1 a_5 \sinh a_5}(1 - \cosh a_5)\right], \tag{41}$$

$$Nu(b_1) = -\frac{b_1 \cos b_1}{\sin b_1}. \tag{42}$$

## V. GRAPHICAL RESULTS AND DISCUSSION

A detailed analysis is made on the effect of MHD mixed convection Poiseuille flow of carbon nanotubes with Casson fluids inside a vertical channel. Both the flow and heat transfer analysis of single and multiple walls CNTs suspended in three different types of base fluids (Water, Kerosene and engine Oil) have been investigated. The governing partial differential equations with associated boundary conditions in non-dimensional form are analyzed for analytic solutions using perturbation method. Solutions for temperature and velocity are obtained on the basis of Xue model.[40] For different parameters, the physics of the problem is discussed graphically and a detailed analysis is performed. The shapes of single and multiple walls carbon nanotubes are given in Fig. 1. Thermophysical properties of base fluids and CNTs are given in Tables II and III provides variation of thermophysical properties of nanofluids with solid volume fraction of CNTs.

### A. Temperature field

The temperature of the flow suffers a notable change with the variation of volume fraction $\phi$ and radiation parameter $N$. The variation in temperature profile with volume fraction and radiation parameter is shown in Figs. 2–4. An increase in temperature is observed with the increase in radiation parameter $N$ for all the three types of base fluids because when $N$ increases it increases conduction from channel to the fluid hence an increase occurs in temperature of the fluid. Temperature increases with the increase in volume fraction. It is due to the fact that thermal conductivity increases with the increase of the addition of solid CNTs which in turn enhances temperature. The temperature of single wall CNTs is greater than multiple wall CNTs. Engine oil/kerosene oil-based nanotubes have greater temperature as compared to water-based nanotubes because of higher thermal conductivity and greater density of water.

### B. Velocity field

The velocity of carbon nanotubes nanofluid is detected to vary more or less with the variation of flow parameters shown graphically. The major factors influencing the velocity are Casson parameter, magnetic and radiation parameter, volume fraction of nanoparticles, Reynolds number and Richardson number. Velocity of MWCNTs is observed to be less than that of SWCNTs. It is due to the fact that

TABLE II. Thermophysical properties of different base fluids and CNTs. (Hone *et al.*[25]; Antar *et al.*[26])

| | Base fluids | | | Nanoparticles | |
|---|---|---|---|---|---|
| Physical properties | Water | Kerosene oil | Engine oil | SWCNT | MWCNT |
| $\rho(kg/m^3)$ | 997 | 783 | 884 | 2,600 | 1,600 |
| $c_p(J/kgK)$ | 4,197 | 2,090 | 1,910 | 425 | 796 |
| $k(W/mK)$ | 0.613 | 0.145 | 0.144 | 6,600 | 3,000 |

TABLE III. Variation of thermophysical properties of nanofluids with solid volume fraction of CNTs.

| SWCNT | $\phi$ | $\rho$ | $\rho c_p(\times 10)$ | $k$ | MWCNT | $\phi$ | $\rho$ | $\rho c_p(\times 10)$ | $k$ |
|---|---|---|---|---|---|---|---|---|---|
| Water | 0 | 997 | 4.167 | 0.613 | Water | 0 | 997 | 4.167 | 0.613 |
| | 0.04 | 1,061 | 4.044 | 1.051 | | 0.04 | 1,021 | 4.051 | 1.011 |
| | 0.08 | 1,125 | 3.921 | 1.528 | | 0.08 | 1,045 | 3.935 | 1.444 |
| Kerosene oil | 0 | 783 | 1.636 | 0.150 | Kerosene oil | 0 | 783 | 1.636 | 0.150 |
| | 0.04 | 855 | 1.615 | 0.274 | | 0.04 | 815 | 1.621 | 0.265 |
| | 0.08 | 928 | 1.593 | 0.410 | | 0.08 | 848 | 1.607 | 0.390 |
| Engine oil | 0 | 884 | 1.688 | 0.144 | Engine oil | 0 | 884 | 1.688 | 0.144 |
| | 0.04 | 952 | 1.665 | 0.264 | | 0.04 | 912 | 1.671 | 0.255 |
| | 0.08 | 1,021 | 1.641 | 0.395 | | 0.08 | 941 | 1.655 | 0.375 |

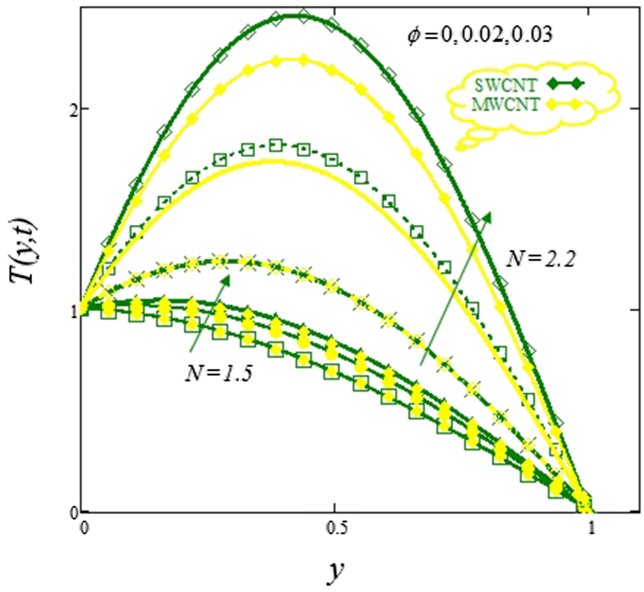


FIG. 2. Temperature profile for different values of $N$ and $\phi$ in water-basednanofluid for SWCNT and MWCNT when $N$ = 1.5, 2.2.

SWCNTs has greater density as well as greater thermal conductivity than MWCNTs which is the factor of enhancement in heat absorption and hence an increases occurs in velocity.

Figures 5–7 highlight the effect of magnetic and Casson parameter simultaneously on velocity profile. Almost identical pattern is observed for single and multiple wall CNTs for the same values of $M$. The behavior of velocity near the channel walls and center is not similar. It shows that for all the three base fluids (Water/Engine oil/kerosene oil), in the absence of magnetic field (that is we considered M=0.000001 very small, negligible value) velocity is higher and it decreases with increases magnetic field. Although, magnetic field can induce current in the conductive fluid, but it create a resistive force namely, Lorentz force which reduces the fluid flow. The velocity is reduced

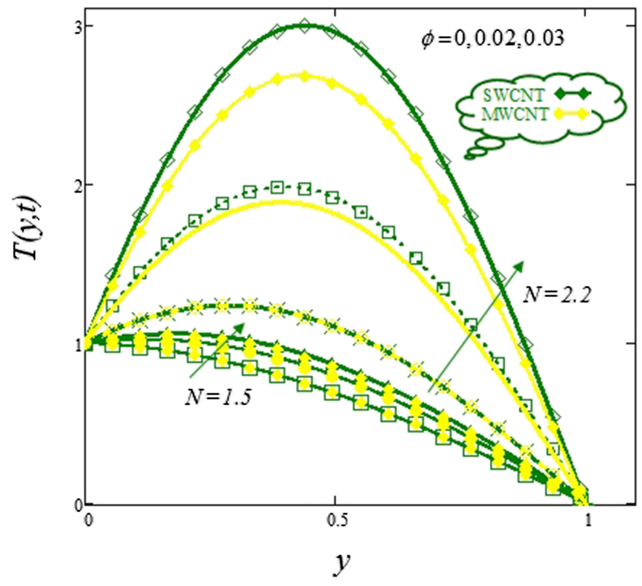


FIG. 3. Temperature profile for different values of $N$ and $\phi$ in engine oil-based nanofluid for SWCNT and MWCNT when $N$ = 1.5, 2.2.

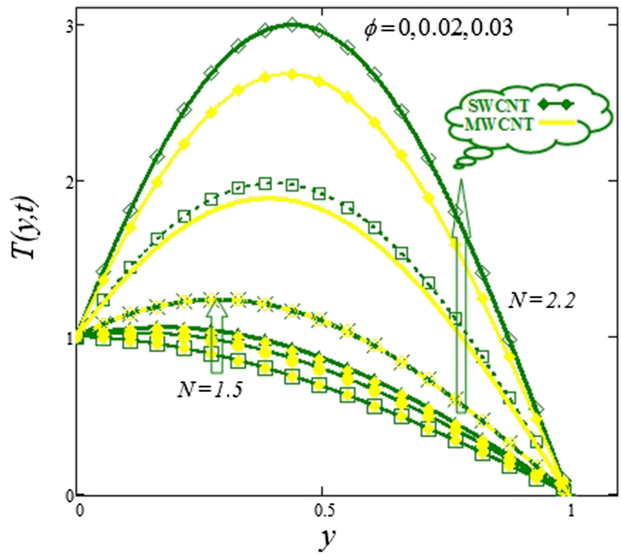


FIG. 4. Temperature profile for different values of $N$ and $\phi$ in kerosene oil-based nanofluid for SWCNT and MWCNT when $N$ = 1.5, 2.2.

under influence of the exterior magnetic field. It is interesting that velocity is maximum along the centerline and minimum at the walls. A similar behavior of $M$ on velocity is observed by Nadeem *et al.*[16] and Aaiza *et al.*[49] Velocity of the fluid increases with increasing values of Casson parameter $\beta$. Casson parameter increases the resistance between the fluid layers hence decreases the flow but here this parameter shows opposite behavior because of absence of MHD which is due to Lorentz force, Also in the presence of magnetic field, an opposite pattern is followed and velocity increases with increasing Casson parameter. Here the influence of Casson parameter shows a decrease in yield stress of the Casson fluid. This facilitates the fluid motion and hence accelerates the flow. The same behavior is observed by Nadeem *et al.*[16] They observed an increase in fluid flow with increase of $\beta$. Moreover, MWCNTs have a bit less velocity than that of SWCNTs. SWCNTs have got greater

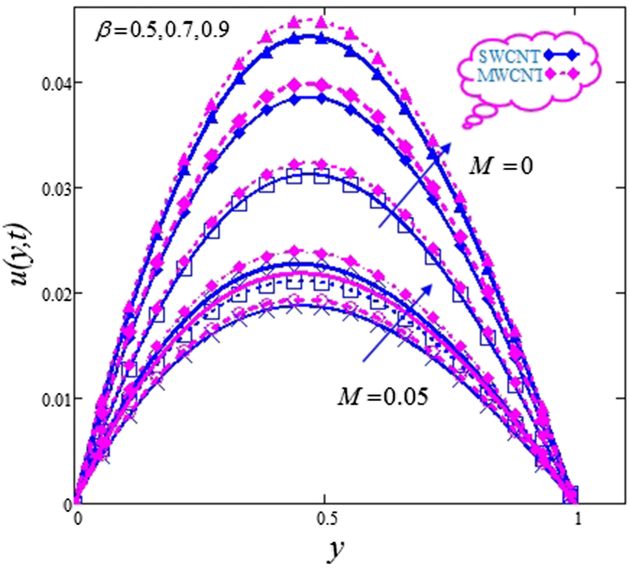


FIG. 5. Velocity profile for different values of $M$ and $\beta$ in water-based nanofluid for SWCNT and MWCNT when $N$ = 1.6, $\phi$ = 0.03, $Re$ = 0.01, $Ri$ = 3.5.

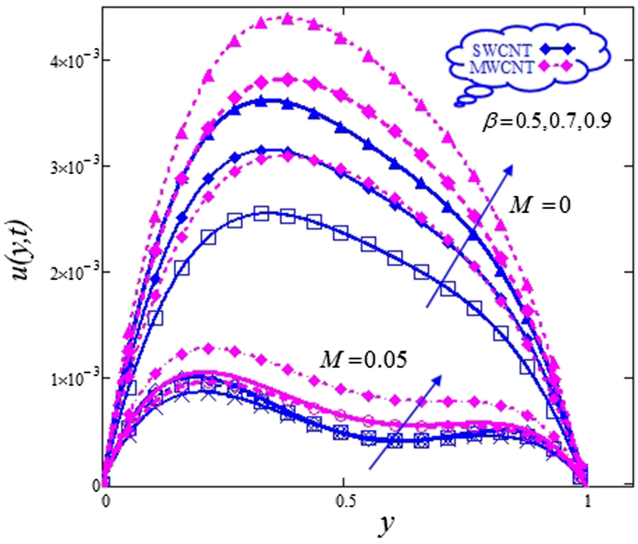


FIG. 6. Velocity profile for different values of $M$ and $\beta$ in Engine oil-based nanofluid for SWCNT and MWCNT when $N = 1.6$, $\phi = 0.03$, $Re = 0.01$, $Ri = 3.5$.

density as compared to MWCNTs but they have greater thermal conductivity as shown in Table II, which leads to enhancement of heat absorption, hence their velocity is greater than MWCNTs. The diameter and length of CNTs also influence their thermal conductivities as Jiang *et al.*[41] found in their work. They found that the thermal conductivities of nano-refrigerant whose diameter is 15*nm* are much higher than those whose diameter is 80*nm*. Smaller diameter means larger specific surface of CNTs and larger specific area stands for more obvious Brownian movement which is an important factor of increasing thermal conductivity of nanofluid. Larger specific area means there are more liquid molecules close to the surface of CNT if volume fraction is same. These liquid molecules can make a layer structure, called Interfacial layer, which can increase their thermal conductivity. Smaller diameter means thicker interfacial layer and greater thermal conductivity enhancement. Similarly for

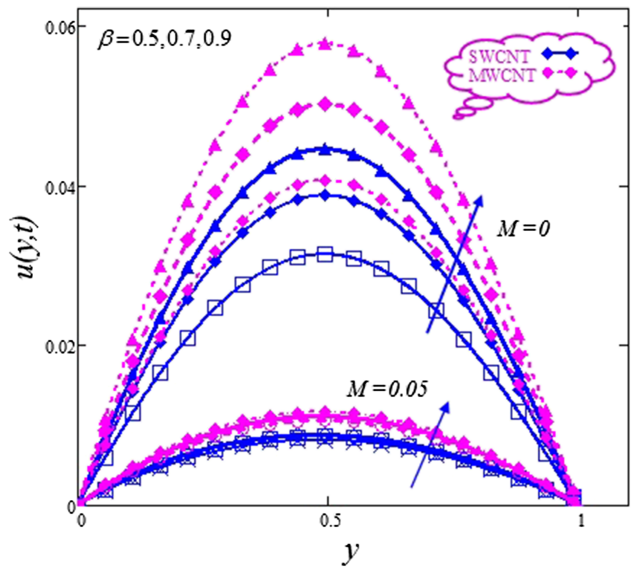


FIG. 7. Velocity profile for different values of $M$ and $\beta$ in kerosene oil-based nanofluid for SWCNT and MWCNT when $N = 1.6$, $\phi = 0.03$, $Re = 0.01$, $Ri = 3.5$.

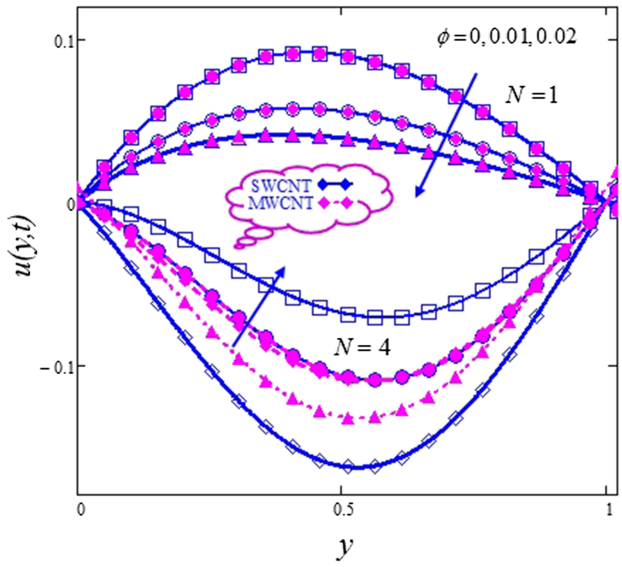


FIG. 8. Velocity profile for different values of $N$ and $\phi$ for water-based nanofluid for SWCNT and MWCNT when $Re = 0.1$, $M = 0.01$, $Ri = 3.5$.

CNTs with same diameters, the larger the aspect ratio of CNT, the higher their thermal conductivity is. But the influence of diameter is more as compared to aspect ratio.

Figure 8–10 show the effect of radiation parameter and volume fraction simultaneously on fluid velocity. In the absence and presence of radiation parameter, velocity decreases with increasing values of volume fraction because the fluid becomes more viscous by adding CNTs but velocity is same for both single and multiple wall carbon nanotubes. Velocity exhibits a decrease by increasing radiation parameter. Velocity for multiple CNTs is less than that of single wall CNTs. At the boundaries velocity is zero for both types of CNTs.

Figure 11–13, illustrates the effect of Reynolds number and Richardson number on velocity profile. It is observed that velocity increases with increase in Reynolds and Richardson number.

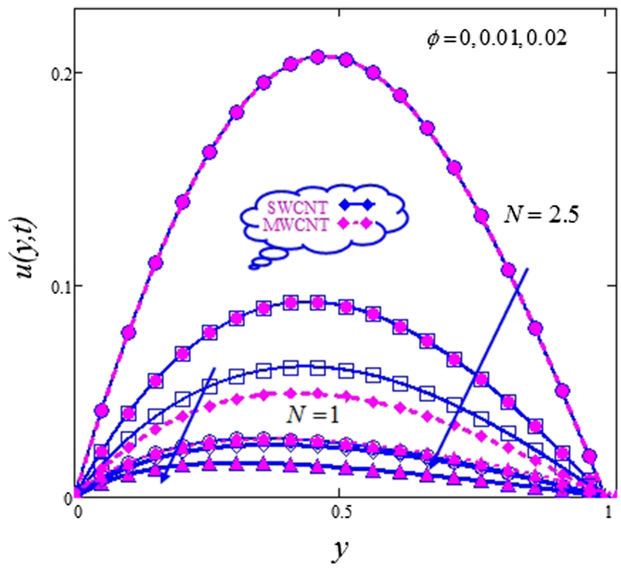


FIG. 9. Velocity profile for different values of $N$ and $\phi$ for engine oil-based nanofluid for SWCNT and MWCNT when $Re = 0.1$, $M = 0.01$, $Ri = 3.2$.

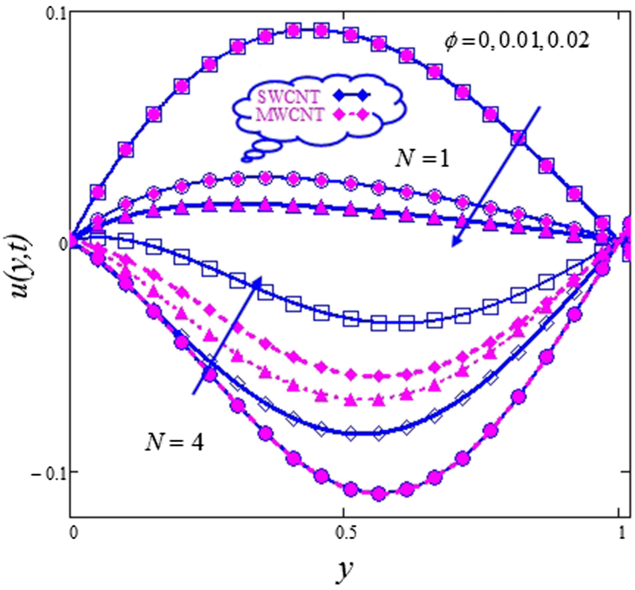


FIG. 10. Velocity profile for different values of $N$ and $\phi$ for kerosene oil-based nanofluid for SWCNT and MWCNT when $Re = 0.1$, $M = 0.01$, $Ri = 3.2$.

Greater Reynolds number stands for greater inertial forces and lesser viscous force making the fluid less viscous thus fluid flows with a greater velocity. Greater Richardson number stands for greater Grashoff number which increase temperature gradiant and buoyancy force (convection), hence leads to an increase in velocity. Velocity of multiple wall CNTs is slightly less than single wall CNTs.

### C. Skin-friction

Table IV shows variation of skin friction values with volume fraction and Casson parameter. It is observed that for water-based SWCNT and MWCNT, skin friction values increase with increasing

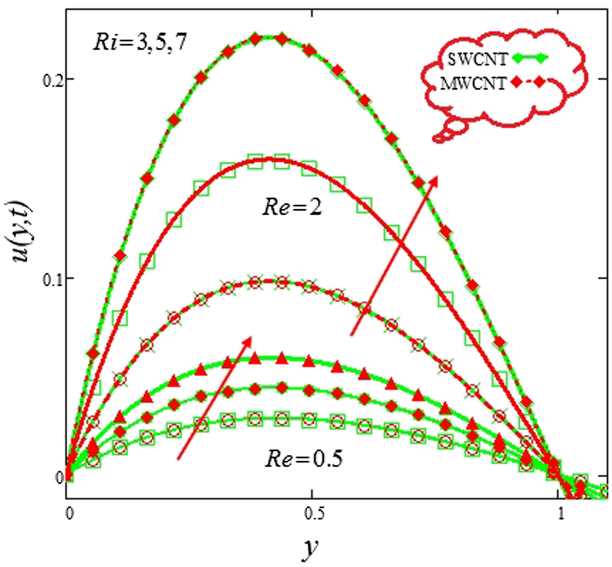


FIG. 11. Velocity profile for different values of $Re$ and $Ri$ for water-based nanofluid for SWCNT and MWCNT when $\phi = 0.04$, $M = 0.025$, $N = 0.8$, $\beta = 0.5$.

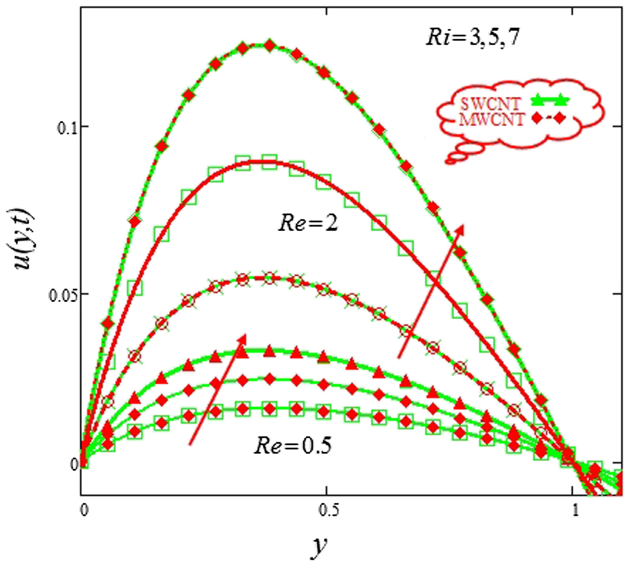


FIG. 12. Velocity profile for different values of *Re* and *Ri* for engine oil-based nanofluid for SWCNT and MWCNT when $\phi = 0.04$, $M = 0.025$, N =1.2, $\beta = 0.5$.

volume Casson parameter and decreases with volume fraction when $\beta = 0.5$. For $\beta = 1,\ 2$ it increases with increasing volume fraction. While skin friction increases with increasing Casson parameter. Thus a regular increase is observed in skin friction with increasing values of $\beta$ and volume fraction. For both types of CNTs of engine and kerosene oil-based nanotubes, skin friction first decreases with increase in volume fraction and then shows an increase with further increase in $\phi$. In the absence of CNTs, skin friction increases with increasing $\beta$ while after adding CNTs, a different behavior is followed. For both types of CNTs skin friction first increases and then decreases for $\beta = 1$ and $\beta = 2$. It is observed that skin friction values are greater for water-based nanotubes than that of Kerosene-oil and Engine-oil nanotubes.

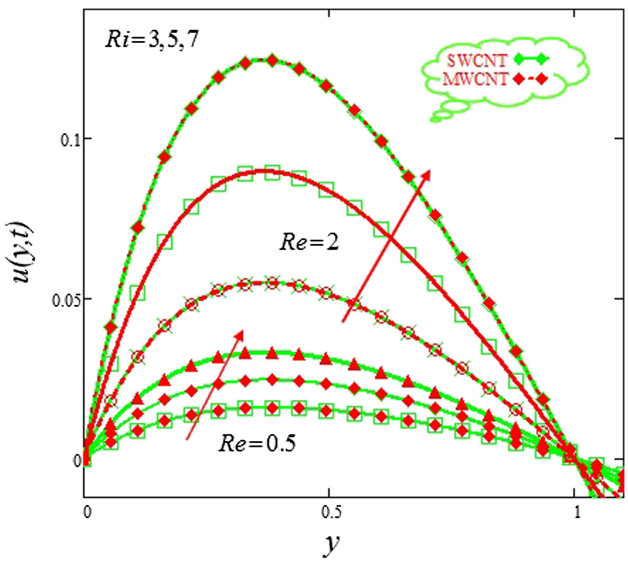


FIG. 13. Velocity profile for different values of *Re* and *Ri* for kerosene oil-based nanofluid for SWCNT and MWCNT when $\phi = 0.04$, $M = 0.01$, $N = 1$, $\beta = 0.5$.

TABLE IV. Variation of Nusselt number and Skin friction with $\phi$ for different values of Casson parameter.

| Water-based | | Skin friction | | | Nusselt number | |
|---|---|---|---|---|---|---|
| SWCNT | $\phi$ | $\beta = 0.5$ | $\beta = 1$ | $\beta = 2$ | $N = 0.5$ | $N = 1.5$ |
| | 0 | 0.073 | 0.109 | 0.146 | -0.195 | -0.106 |
| | 0.02 | 0.064 | 0.096 | 0.125 | -0.885 | 0.304 |
| | 0.04 | 0.057 | 0.082 | 0.106 | -0.853 | 0.817 |
| MWCNT | 0 | 0.073 | 0.109 | 0.146 | -0.915 | -0.106 |
| | 0.02 | 0.064 | 0.094 | 0.123 | -0.888 | 0.263 |
| | 0.04 | 0.057 | 0.082 | 0.106 | -0.859 | 0.717 |
| Kerosene-based | | | | | | |
| SWCNT | 0 | 0.073 | 0.109 | 0.146 | -0.195 | -0.106 |
| | 0.02 | 0.056 | 0.079 | 0.099 | -0.88 | 0.38 |
| | 0.04 | 0.046 | 0.061 | 0.075 | -0.842 | 1.011 |
| MWCNT | 0 | 0.073 | 0.109 | 0.146 | -0.915 | -0.106 |
| | 0.02 | 0.056 | 0.078 | 0.097 | -0.882 | 0.338 |
| | 0.04 | 0.046 | 0.061 | 0.075 | -0.848 | 0.903 |
| Engine oil | | | | | | |
| SWCNT | 0 | 0.073 | 0.109 | 0.146 | -0.915 | -0.106 |
| | 0.02 | 0.056 | 0.079 | 0.099 | -0.88 | 0.38 |
| | 0.04 | 0.046 | 0.061 | 0.074 | -0.842 | 1.012 |
| MWCNT | 0 | 0.073 | 0.109 | 0.146 | -0.915 | -0.106 |
| | 0.02 | 0.056 | 0.078 | 0.097 | -0.882 | 0.338 |
| | 0.04 | 0.046 | 0.061 | 0.074 | -0.848 | 0.904 |

### D. Rate of heat transfer

Different values of Nusselt numbers which measures the rate of heat transfer are shown in Table IV. Heat transfer rate increases with volume fraction $\phi$ and radiation parameter $N$, its different values are shown in Table IV. The same pattern is followed for both types of CNTs and all the three base fluids (water/kerosene-oil/Engine-oil). Nusselt number is the ratio of convection to conduction so here it means that convection increases with increase in $\phi$ and radiation parameter. As by adding more CNTs in the base fluid, increases its thermal conductivity and hence heat transfer get enhanced.

## VI. CONCLUSIONS

In this attempt, the effect of single and multiple wall CNTs on the thermal conductivity of Casson nanofluids is observed in the presence of MHD where water/kerosene-oil/Engine-oil was used as base fluids. The governing equations are formulated, non-dimensionalized and then solved by perturbation technique.

We came up with the following outcomes:

- ➢ Increase in volume fraction causes a decrease in velocity of the fluid as the nanofluid becomes more viscous by adding CNTs.
- ➢ Velocity increases with increase in Reynolds number and Richardson number because of greater Grashoff number (thermal bouncy force) and less viscous forces.
- ➢ Velocity increase with increase in radiation parameter due to increase in heat transfer to the fluid.
- ➢ Temperature increases with increase in radiation parameter and volume fraction because of enhancement in thermal conductivity.
- ➢ The temperature of single wall CNTs is greater than multiple wall CNTs for all the three base fluids.
- ➢ Engine oil and kerosene oil-based nanotubes have greater temperature as compared to water-based nanotubes because water has a greater density.

- ➢ Rate of heat transfer increases with increase in radiation parameter and volume fraction because of enhancement in thermal conductivity.
- ➢ Skin friction decreases with increasing volume fraction for small values of $\beta$ while increases with volume fraction for $\beta = 1, 2$.
- ➢ Skin friction values for water-based nanotubes is greater as compared to kerosene oil and engine oil-based nanotubes.
- ➢ The thermal conductivity of CNTs nanofluids increases with volume fraction of CNTs as well as with their diameter and length.

## ACKNOWLEDGMENTS

The authors acknowledge with thanks the Deanship of Scientific Research (DSR) at Majmaah University, Majmaah and at the Deanship of Scientific Research (DSR) King Abdul Aziz University, Jeddah Saudi Arabia for technical and financial support.
Authors confirm that there is no conflict of interest.

[1] N. Casson, *A Flow Equation for Pigment-Oil Suspensions of the Printing Ink Type, Rheology of Disperse Systems* (pergamon press, London, UK, 1959).
[2] R. K. Dash, K. N. Mehta, and G. Jayaraman, "Casson fluid flow in a pipe filled with a homogenous porous medium," Int J Eng. sci. **34**(10), 1145–56 (1996).
[3] N. T. M. Eldabe and M. M. G. E. Salwa, "Heat transfer of MHD non-Newtonian Casson fluid flow between two rotating cylinder," J Phys Soc Jpn **64**, 41–64 (1995).
[4] J. Boyd, J. M. Buick, and S. Green, "Analysis of the Casson and carreau-yasuda non-Newtonian blood models in steady and oscillatory flow using the lattice. Boltzman method," Phys Fluids **19**, 93–103 (2007).
[5] M. Swati, D. R. Pravita, and B. Krishnendu, "Casson fluid over an unsteady stretching surface," Ain Shams Engineering Journal **4**, 933–938 (2013).
[6] S. Pramanik, "Casson fluid flow and heat transfer past an exponentially porous stretching surface in presence of thermal radiation," Ain Shams Engineering Journal **5**, 205–212 (2014).
[7] A. S. Noreen, "Influence of magnetic field on peristaltic flow of a Casson fliud in an asymmetric channel: Application in crude oil refinement," Journal of Magnetism and Magnetic Materials **378**, 463–468 (2015).
[8] A. Farhad, I. Khan, and S. Sharidan, "Closed form solutions for unsteady free convection flow of a second grade fluid over an oscillating vertical plate," PLoS ONE **9**(2) (2014).
[9] A. Hussanan, M. Z. Salleh, R. M. Tahar, and I. Khan, "Unsteady boundary layer flow and heat transfer of a Casson fluid past an oscillating vertical plate with Newtonian heating," PloS One **9**(10), e108763 (2014).
[10] K. Asma, I. Khan, K. Arshad, and S. Sharidan, "Unsteady MHD free convection flow of Casson fluid past over an oscillating vertical plate embedded in a porous medium," Engineering Science and Technology, an International Journal **18**, 309–317 (2015).
[11] M. A. Imran, S. Sarwar, and M. Imran, "Effects of slip on free convectionflow of Casson fluid over an oscillating vertical plate," Boundary Value Problems 30–41 (2016).
[12] C. S. K. Raju, N. Sandeep, V. Sugunamma, M. J. Babu, and J. V. R. Reddy, "Heat and mass transfer in magnetohydrodynamic Casson fluid over an exponentially permeable stretching surface," Engineering Science and Technology, an International Journal **19**, 45–52 (2016).
[13] F. Gentile, M. Ferrari, and P. Decuzzi, "The transport of nanoparticles in blodd vessels: The effect of vessel permeability and blood rheology," Annals of Biomedical Engineering **36**(2), 254–261 (2007).
[14] H. U. Rizwan, S. Nadeem, K. H. Zafar, and O. G. Toyin, "Convective heat transfer and MHD effects on Casson nanofluid flow over a shrinking sheet," Central Europeon Journal Journal of Physics **12**, 862–871 (2014).
[15] A. M. Siddiqui, A. A. Farooq, and M. A. Rana, "A mathematical model for the flow of a Casson fluid due to metachronal beating of cilia in a tube," The Science World Journal (2015), ID: 487819 J.
[16] S. Nadeem, R. U. Haq, and A. S. Noreen, "MHD three-dimensional boundary layer flow of Casson nanofluid past a linearly stretching sheet with convective boundary condition," IEEE Transaction on Nanotechnology **13**, 109–115 (2014).
[17] K. Bhattacharyya, "MHD stagnation-point flow of Casson fluid and heat transfer over a stretching sheet with thermal radiation," Journal of Thermodynamics (2013), ID: 169674.
[18] A. Walicka and J. Falicki, "Reynolds number effects in the flow of an electro rheological fluid of Casson type between fixed surface of revolution," Appl. Math. Compt. **250**, 639–649 (2015).
[19] G. Sarojamma and K. Vendabai, "Boundary layer flow of a Casson nanofluid past a vertical exponential stretching cylinder in the presence of a transverse magnetic field with internal heat generation/absorption," Int. J. Mech. Aaerosp. Ind. Mechatr. Eng. **9**(1), (2015).
[20] M. Mustafa and K. A. Junaid, "Model for flow of Casson nanofluid past a non-linearly stretching sheet considering magnetic field effects," AIP Advances **5**, 077148 (2015).
[21] M. S. Liu, M. C. C. Lin, H. I-Te, and C. C. Wang, "Enhancement of thermal conductivity with carbon nanotube for nanofluids," Int. Comm. in Heat and Mass Transfer **32**, 1202–1210 (2005).
[22] F. D. S. Marquis and L. P. F Chibnate, "Improving the heat transfer of nanofluids and nanolubricants with Carbon nanotubes," JOM 32–43 (2005).
[23] D. Wen and Y. Ding, "Effective thermal conductivity of aqueous suspensions of carbon nanotubes," Journal of Thermophysics and Heat Transfer **18**(4), 481–485 (2004).

[24] H. Xie, H. Lee, and M. Choi, "Nanofluids containing multiwall carbon nanotubes and their enhanced thermal conductivities," J. Appl. Phys. **94**, 4967–4971 (2003).
[25] J. Hone, M. C. Llaguno, M. J. Biercuk, A. T. Johnson, B. Batlogg, Z. Benes, and J. E. Fischer, "Thermal properties of carbon nanotubes and nanotube-based material," Appl. Phys. A **74**, 339–343 (2002).
[26] Z. Antar, H. Noel, J. F. Feller, P. Glouannec, and K. Elleuch, "Thermophysical and radiative properties of conductive biopolymer composite," Matter Sci Forum **714** 115–122 (2012).
[27] S. T. Hussain, R. U. Haq, Z. H. Khan, and S. Nadeem, "Water driven flow of carbon nanotubes in a rotating channel," Journal of Molecular Liquids **214**, 136–144 (2016).
[28] W. A. Khan, Z. H. Khan, and M. Rahi, "Fluid flow and heat transfer of carbon nanotubes along a flat plate with Navier slip boundary," Appl Nanosci **4**, 633–641 (2014).
[29] R. U. Haq, S. Nadeem, Z. H. Khan, and N. F. M. Noor, "Convective heat transfer in MHD slip flow over a stretching surface in the presence of carbon nanotubes," Phys. B Condens. Matter **457**, 40–47 (2015).
[30] R. U. Haq, Z. H. Khan, and W. A. Khan, "Thermophysical effects of carbon nanotubes on MHD flow over a stretching surface," Phys. E: Low Dimens. Sys. Nanostruct. **63**, 215–222 (2014).
[31] L. Xiao, Z. Chin, C. Feng, L. Liu, Z.-Q. Bai, Y. Wang, L. Qian, Y. Zhang, Q. Li, K. Jiang, and S. Fan, "Flexible, stretchable,transparent carbon nanotube thin film loudspeakers," Nanoletters **12**(8), 4539–4545 (2008).
[32] L. Camilli, C. Pisani, E. Gautron, M. Scarselli, P. Castrucci, F. D. Orazio, M. Passacantando, D. Moscone, and M. De. Crescenzi, "A three-dimensional carbon nanotube network for water treatment," Nanotechnology **25** (2014).
[33] S. Halelfadl, P. Estelle, B. Aladag, N. Doner, and T. Mare, "Viscosity of carbon nanotubes water-based nanofluids: Influence of concentration and temperature," Interantional Journal of Thermal Sciences **71**, 111–117 (2013).
[34] S. Halelfadi, T. Mare, and P. Estelle, "Efficiency of carbon nanotubes water based nanofluids as coolants," Experimental Thermal and Fluid Science **53**, 104–110 (2014).
[35] R. Kamli and A. Binesh, "Numerical investigation of heat transfer enhancement using carbon nanotube-based non-newtonian nanofluids," Int. Commun. Heat Mass Transfer **37**(8), 1153–1157.
[36] J. Mayer, T. Mckrell, and K. Grote, "The influence of multi-walled carbon nanotubes on single-phase heat transfer and pressure drop characteristics in the transitional flow regime of smooth tubes," Int. J. Heat Mass Transfer **58**(1-2), 597–609 (2013).
[37] R. Kandasamy, R. Mohamad, and M. Ismoen, "Impact of chemical reaction on Cu, Al2O3, and SWCNTs-nanofluid flow under slip conditions," Engineering Science and Technology, an International Journal (2015).
[38] R. Kandasamy, I. Muhaimin, and R. Mohammad, "Single walled carbon nanotubes on MHD unsteady flow over a porous wedge with thermal radiation with variable stream conditions," Alexandria Engineering Journal **55**, 275–285 (2016).
[39] X.-H. Ren, J.-T. Ho, D. Liu, F.-Y. Zhao, X.-H. Li, and H.-Q. Wang, "Combined convective heat and airborne pollutant removals in a slot vented enclosure under different flow schemes: parametric investigations and non unique flow solutions **94**, 159–169 (2015).
[40] Q. Xue, "Model for thermal conductivity of carbon nanotube-based composites," Phys B condens Matter **368**, 302–307 (2005).
[41] W. Jiang, G. Ding, and H. Pang, "Measurement and model on thermal conductivities of carbon nanotube nanorefrigerants," International Journal of Thermal Sciences **48**, 1108–1115 (2009).
[42] K. Al-Salem, H. F. Oztop, I. Pop, and Y. Varol, "Effect of moving lid direction on MHD mixed convection in a linearly heated cavity," International Journal of Heat and Mass Transfer **55**, 1103–1112 (2012).
[43] K. V. Prasad, K. Vajravelu, and P. S. Datti, "The effect of variable fluid properties on the MHD flow and heat transfer over a non-linear stretching sheet," International Journal of Thermal Science **49**, 603–610 (2010).
[44] S. Sebdani, M. Mahmoodi, and S. Hashemi, "Effect of nanofluid variable properties on mixed convection in a square cavity," International Journal of Thermal Sciences **52**, 112–126 (2012).
[45] R. K. Tiwari and M. K. Das, "Heat transfer augmentation in a two-sided lid-driven differentially heated square cavity utilizing nanofluids," International Journal of Heat and Mass Transfer **50**, 9–10 (2007).
[46] G. A. Sheikhzadeh, N. Hajialigol, M. E. Qomi, and A. Fattahi, "Laminar mixed convection of Cu-water nano-fluid in two sided lid-driven enclosures," Journal of Nanostructures **1**, 44–53 (2012).
[47] T. Fan, H. XU, and I. Pop, "Mixed convection heat transfer in horizontal channel filled with nanofluids," International Journal of springer plus **34**, 339–350 (2013).
[48] A. Khalid, I. Khan, and S. Sharidan, "Exact solutions for free convection flow of nanofluids with ramped wall temperature," The European Physical Journal Plus **130**, 57–71 (2015).
[49] G. Aaiza, I. Khan, S. Sharidan, A. Khalid, and A. Khan, "Heat transfer in MHD mixed convection flow of a ferrofluid along a vertical channel," PLoSONE **10**(11), e0141213 (2015).
[50] G. Aaiza, I. Khan, and S. Shafi, "Energy transfer in mixed convection MHD flow of nanofluid containing different shapes of nanoparticles in a channel filled with saturated porous medium," Nanoscale Research Letters.
[51] J. C. Maxwell, *Electricity and magnetism*, 3rd ed. (clarendon, Oxford, 1904).
[52] D. J. Jaffery, "conduction through a random suspension of spheres," Proc Roy soc Lond ser A Math Phys Sci **335**, 335–367 (1973).
[53] R. Davis, "The effective thermal conductivity of a composite material with spherical inclusions," Int J Thermophys **7**, 609–620 (1986).
[54] R. L. Hamilton and O. K. Crosser, "Thermal conductivity of heterogenous two-component systems," Ind Eng Chem Fund **1**(3), 187–191 (1962).
[55] S. Choi, and J. Eastman, "Enhancing thermal conductivity of fluids with nanoparticles," in The proceedings of 1995 ASME (1995).